# Rab28 function in trypanosomes: interactions with retromer and ESCRT pathways

**Jennifer H. Lumb*, Ka Fai Leung, Kelly N. DuBois and Mark C. Field‡**

Department of Pathology, University of Cambridge, Tennis Court Road, Cambridge CB2 1QP, UK

*Present address: Cambridge Institute for Medical Research, MRC/Wellcome Trust building, Addenbrooke's Hospital, Hills Road, Cambridge CB2 0XY, UK
‡Author for correspondence (mcf34@cam.ac.uk)

*Accepted 1 July 2011*
*Journal of Cell Science 124, 3771–3783*

*doi: 10.1242/jcs.079178*

## Summary

Early endosomal cargo is typically targeted to either a degradative or recycling pathway. Despite established functions for the retromer and ESCRT complexes at late endosomes/multivesicular bodies, the mechanisms integrating and coordinating these functions remain largely unknown. Rab family GTPases are key membrane trafficking organizers and could contribute. Here, in the unicellular organism *Trypanosoma brucei*, we demonstrate that Rab28 locates to the endosomal pathway and partially colocalizes with Vps23, an ESCRT I component. Rab28 is required for turnover of endocytosed proteins and for lysosomal delivery of protein cargo. Using RNA interference we find that in Rab28-depleted cells, protein levels of ESCRT I (Vps23/28) and retromer (Vps26) are also decreased, suggesting that Rab28 is an important regulator of these factors. We suggest that Rab28 coordinates the activity of retromer-dependent trafficking and ESCRT-mediated degradative pathways.

**Key words:** Rab28, ESCRT, Retromer, Endocytosis, Trypanosome, Vesicle transport

## Introduction

Membrane trafficking requires temporal and spatial coordination to ensure that molecules reach their correct destinations. In animals, fungi and multicellular plants, this system is highly flexible and facilitates responses to environmental and developmental changes. Rab (Ras-related proteins in brain) GTPases regulate membrane trafficking and function in many transport steps (Seabra et al., 2002; Behnia and Munro, 2005). In the GTP-bound form, Rabs are deployed to membranes and recruit effector molecules involved in vesicle formation, cytoskeletal-dependent transport, tethering and fusion with destination organelles (Grosshans et al., 2006). Rabs are regulated by multiple proteins, including GTPase-activating proteins (GAPs) and guanine exchange factors (GEFs), making them pivotal for coordinating membrane transport (Stenmark, 2009; Brighouse et al., 2010).

Rab28 is a divergent member of the Rab family, with lower sequence identity against canonical Rab proteins (31–33%) than is typical (>40%) (Brauers et al., 1996; Pereira-Leal and Seabra, 2001), and also with little homology beyond the GTP-binding site and divergence within phosphate-binding regions. Conserved residues in Rab switch/interswitch regions bind many proteins, including GAPs, GEFs and effectors (Eathiraj et al., 2005; Ostermeier and Brunger, 1999; Delprato and Lambright, 2007; Merithew et al., 2001); significantly, the WDTAGQE motif in Rab28 is diverged to WDIGGQT. Further, the switch domain in human RAB28 undergoes a greater conformational change between GTP and GDP states than other Rab proteins (Lee et al., 2008). Two Rab28 splice variants that differ at their C-termini are present in mammals. The short isoform is ubiquitously expressed and the long isoform restricted to testes (Brauers et al., 1996). Human RAB28 contains an S[D/E][D/E]E motif within the unstructured N-terminal domain, which binds BARD1, an interaction partner of the breast cancer gene product BRCA1 (Irminger-Finger et al., 2006). However the role of Rab28 in endomembrane trafficking remains undefined.

Multivesicular bodies (MVBs) are late endosomal sorting compartments. Ubiquitylated proteins destined for lysosomal degradation are concentrated into intralumenal budding vesicles by the endosomal sorting complex required for transport (ESCRT complex), whereas resident proteins and those destined for retrograde transport are retained within the limiting membrane (Felder et al., 1990; van Deurs et al., 1993; Wollert and Hurley, 2010). The retromer VPS26–VPS29–VPS35 subcomplex selects cargo destined for the Golgi complex into outwardly budding tubules generated by sorting nexins (SNXs) (Arighi et al., 2004; Seaman, 2004). Retromer and ESCRT complex activities must be tightly coordinated but the regulatory mechanism(s) responsible are unknown.

*Saccharomyces cerevisiae* lacks Rab28, so we selected *Trypanosoma brucei* as an alternative model. *T. brucei* is experimentally tractable and a member of the Euglenozoa, a group suggested to be close to the eukaryotic evolutionary root, with a well-characterized endomembrane system (Cavalier-Smith, 2010; Field and Carrington, 2009). Trypanosomes have an ordered organellar anatomy with endocytosis and exocytosis restricted to an invagination of the plasma membrane, the flagellar pocket. Clathrin-mediated endocytosis is the sole uptake mechanism and endocytosis is developmentally regulated (Langreth and Balber, 1975; Morgan et al., 2001; Allen et al., 2003; Hung et al., 2004; Jeffries et al., 2001).

We demonstrate that *T. brucei* Rab28 partially colocalizes with vacuole protein sorting 23 (Vps23) and that it participates in endocytic transport pathways. Using RNA interference (RNAi) we find that Rab28 mediates maintenance of the Golgi complex

and maintains expression levels and locations of retromer and ESCRT complex subunits. These data suggest Rab28 functions in coordinating late endocytic events.

## Results

### *T. brucei* Rab28 is a novel endocytic protein

We examined the role of the *T. brucei* orthologue of mammalian Rab28 in membrane transport. *T. brucei* offers an attractive system in which to study this Rab protein on account of a streamlined endocytic system coupled to a high level of definition, together with extensive evidence that Rab orthologues maintain broadly similar functions across deep evolutionary time (Field and Carrington, 2009; Brighouse et al., 2010). *T. brucei* Rab28 (Tb927.6.3040) was initially identified by comprehensive screening of the trypanosome genome for Ras- and Rab-like small GTPases (Berriman et al., 2005; Ackers et al., 2005); *T. brucei* Rab28 shares 49% identity and 58% similarity to *H. sapiens* RAB28 and extensive similarity to orthologues in other taxa, notably within the C-terminal hypervariable domain. Rab28 is widely distributed across the Eukaryota, despite secondary losses resulting in the absence of Rab28 from Plantae, Fungi and Amoebozoa, and therefore Rab28 is dispensable in certain organisms (Lumb and Field, 2011). To examine *T. brucei* Rab28 expression in trypanosomes we initially analyzed mRNA levels; quantitative real time PCR (qRT-PCR) confirmed Rab28 transcripts in both bloodstream form (BSF) and procyclic form (PCF) trypanosomes, suggesting a role throughout the life cycle (Fig. 1A).

To determine subcellular location, *T. brucei* Rab28 was fused to an N-terminal haemagglutinin (HA) or YFP-epitope tag and ectopically expressed in BSF cells. Production of the respective chimeras, TbRab28HA (31 kDa) and TbRab28YFP (51 kDa), of the correct molecular weight were verified by western blotting (Fig. 1B). Indirect immunofluorescence analysis (IFA) on cells expressing TbRab28HA and TbRab28YFP detected discrete puncta in the cytoplasm posterior to the nucleus and anterior to the kinetoplast. No such staining was seen in non-transfected cells (Fig. 1D). Rab28-positive structures replicated following kinetoplast segregation and were partitioned between daughter cells (Fig. 1E). To verify the location of *T. brucei* Rab28, we raised antibodies against a GST::*T. brucei* Rab28 fusion protein in rabbits. The specificity of affinity-purified antibody was validated by western blot, and IFA recapitulated the distribution of tagged Rab28 proteins in BSF cells (Fig. 1C,F). This antibody proved to be highly labile and hence could not be used in subsequent analyses. However, the distinct location, highly similar to endogenous *T. brucei* Rab28 for both the HA and YFP chimeras, argued strongly for a location of Rab28 between the kinetoplast and nucleus. When equivalent Rab28 chimeras were expressed in PCFs, the localization was essentially indistinguishable from BSF, which suggested that the location of *T. brucei* Rab28 is maintained between developmental stages (Fig. 1G).

### Subcellular location of *T. brucei* Rab28

The region between the nucleus and kinetoplast in trypanosomes contains the flagellar pocket, endosomes, the lysosome and the Golgi complex, a crowded region that makes fine discrimination between membraneous subcompartments challenging (Field and Carrington, 2009). However, the location of *T. brucei* Rab28 was consistent with association with one or more of these compartments, especially the endosomes and lysosome (Field et al., 1998; Jeffries et al., 2001; Gabernet-Castello et al., 2009; Leung et al., 2008; Alexander et al., 2002).

We attempted to identify the subcellular location of *T. brucei* Rab28 more clearly using a combination of wide field and confocal immunofluorescence microscopy, the latter to eliminate potential colocalization in the *x*-*y* plane but distinct location in the *z*-axis (Fig. 2A). Cells ectopically expressing Rab28 were co-stained with antibodies against a validated panel of markers for trypanosome intracellular compartments. We found little colocalization between *T. brucei* Rab28 and the clathrin heavy chain, despite very close apposition of the membranes. *T. brucei* Rab28 appeared distinct from Rab5A, Rab5B and Rab11, with essentially no colocalization, despite a presence on structures that are extremely close to each other. Furthermore, *T. brucei* Rab28 and GRASP are completely distinct. Therefore, we conclude that Rab28 has essentially no steady-state presence on the Golgi complex, clathrin-containing compartments, or early and recycling endosomes.

There was some colocalization with p67, suggesting that *T. brucei* Rab28 might have a presence on lysosomal or pre-lysosomal membranes (Kelley et al., 1999). Furthermore, Rab28 partly colocalizes with HA-tagged Vps23, an ESCRT I component (Leung et al., 2008; Katzmann et al., 2001; Babst et al., 2000), and to a lesser extent with the retromer subunit, Vps26 (Shorter et al., 1999; Seaman et al., 1998). In summary, these data suggest that *T. brucei* Rab28 locates close to multiple endosomal constituents but specifically associates more substantially with Vps23-positive structures. By analogy to mammalian cells, these data suggest a presence for *T. brucei* Rab28 on structures similar to late endosomes and pre-lysosomes. To exclude potential overexpression artefact we also tagged *T. brucei* Rab28 at the N-terminus in situ, i.e. in the endogenous genomic location (Kelly et al., 2007) (Fig. 2B). In situ *T. brucei* Rab28 also demonstrated association with Vps23, which was essentially indistinguishable from the ectopically expressed Rab28 localization (Fig. 2A). Higher definition assignment of *T. brucei* Rab28 is not possible using confocal microscopy due to the extremely close apposition of the organelles and the small volume of the trypanosome cytoplasm in this region.

### *T. brucei* Rab28-depleted cells exhibit trafficking defects

RNAi is highly efficient in trypanosomes, and especially resistant to off-target effects (Koumandou et al., 2008). Moreover co-suppression requires high sequence similarity, and specific knockdown of trypanosomatid genes sharing over 60% identity has been achieved without off-target effects (Bastin et al., 2000); *T. brucei* Rab28 is 27% identical to its closest paralogue, Rab23. A plasmid allowing tetracycline (TET)-inducible expression of Rab28 double-stranded RNA was used to generate a *T. brucei* Rab28$^{RNAi}$ line. Knockdown was validated by both northern blot and western blot on a Rab28$^{RNAi}$ mutant ectopically expressing TbRab28HA. Expression of *Rab28* mRNA and protein was rapidly suppressed by ~90% after 24 hours, whereas BiP levels remained unchanged, indicating that RNAi was specific (Fig. 3A,B).

A significant and reproducible impact on proliferation of BSF cells was obtained within 48 hours of inducing *T. brucei* Rab28$^{RNAi}$ cells (Fig. 3C), indicating that Rab28 is required for normal cellular function. By day 3, the propagation rate of

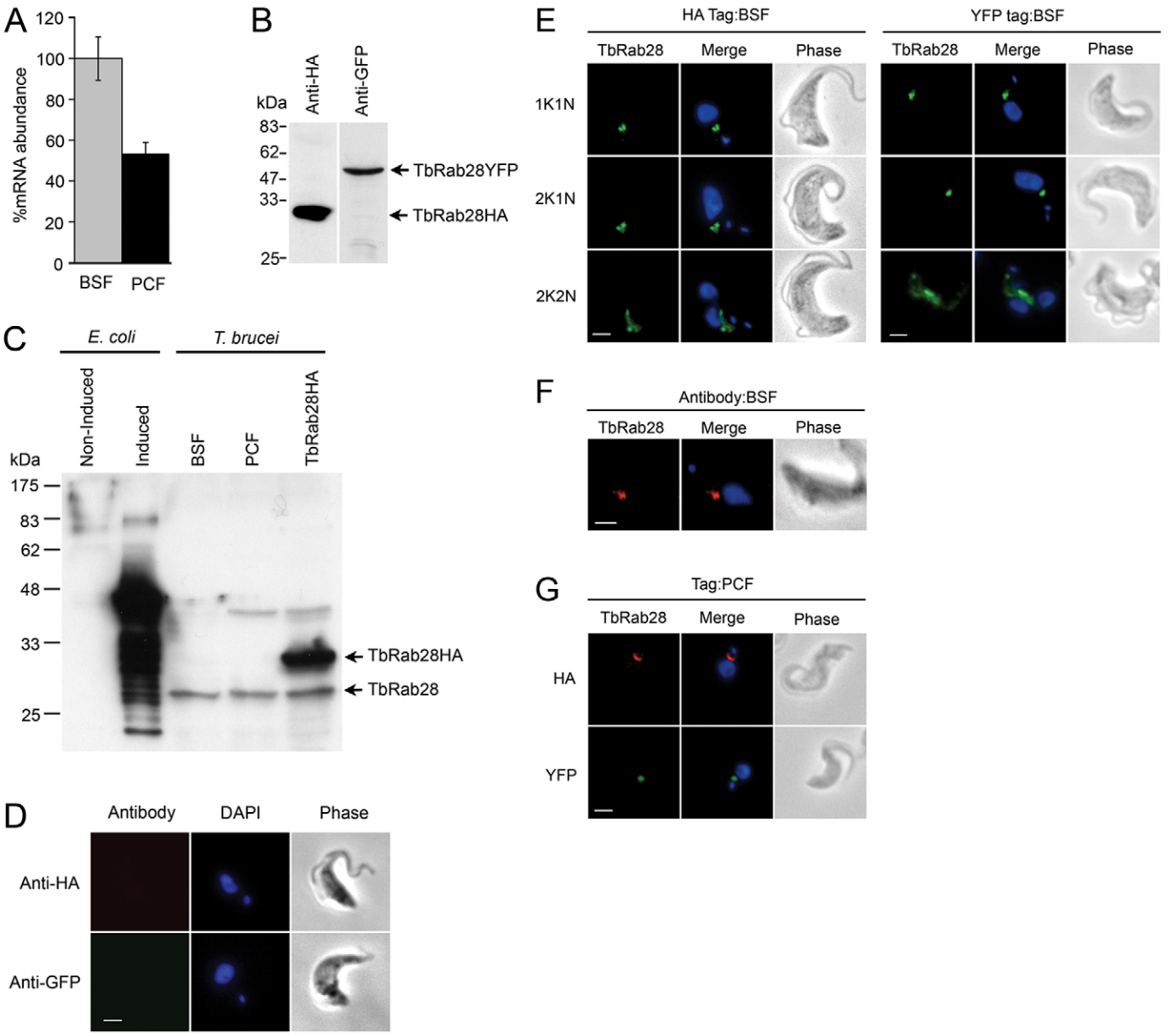


**Fig. 1. Expression of *T. brucei* Rab28 and validation of antibodies.** (**A**) *Rab28* mRNA is expressed at similar levels in BSF and PCF cells. Data were normalized for RNA input to β-tubulin and expression of *Rab28* mRNA in PCF calibrated against expression in BSF. Errors bars show s.e.m. from triplicate RNA extractions (**B**) Production of TbRab28HA (29 kDa) and TbRab28YFP (51 kDa) proteins of the correct size in trypanosomes was verified by western blot using anti-HA or anti-GFP on transfected BSF cells. (**C**) Western blot of purified anti-serum (1:1000) against *T. brucei* Rab28 on bacterial (10 ng) and cell ($10^7$ cells) lysates. 'Induced' denotes bacterial whole cell lysate in which expression of recombinant GST::*T. brucei* Rab28 was induced. *T. brucei* Rab28 antibodies recognized an antigen of 48 kDa corresponding to GST::*T. brucei* Rab28 that was absent in non-induced culture. An antigen (27 kDa) similar to the predicted size of *T. brucei* Rab28 (26 kDa) was recognized in BSF and PCF. Presence of endogenous Rab28 in addition to an antigen of 31 kDa corresponding to TbRab28HA (29 kDa) was detected in recombinant *T. brucei* Rab28 cells. (**D**) Immunofluorescence images of wild-type SMB BSF cells (Lister 427) stained with antibodies to HA and GFP. Cells were stained with anti-HA and counterstained with Alexa Fluor 568 or with anti-GFP and counterstained with Oregon Green. DNA was visualized with DAPI (blue). Anti-HA and anti-GFP did not cross-react with trypanosome structures, validating the use of these antibodies in subsequent localization experiments. (**E**) Location of Rab28 during the BSF cell cycle. Cells were transfected for expression of N-terminal HA- or YFP-tagged Rab28 and the tagged protein visualized with anti-HA (left panel) or anti-GFP (right panel). DNA in all figures is co-stained with DAPI (blue). 1K1N signifies G1 phase, 2K1N early nuclear S-phase; and 2K2N that the kinetoplast replicates prior to the nucleus. *T. brucei* Rab28 locates between the nucleus and kinetoplast. Rab28 localization becomes more extensive at G2. (**F**) Representative image of endogenous Rab28 in BSF cells. Cells were stained with anti-*T. brucei* Rab28 and counterstained with Alexa Fluor 568 (red). (**G**) Location of Rab28 in PCF cells. HA- and YFP-tagged Rab28 were expressed in PCF cells and visualized with antibodies. Representative images are shown. Scale bars: 2 µm.

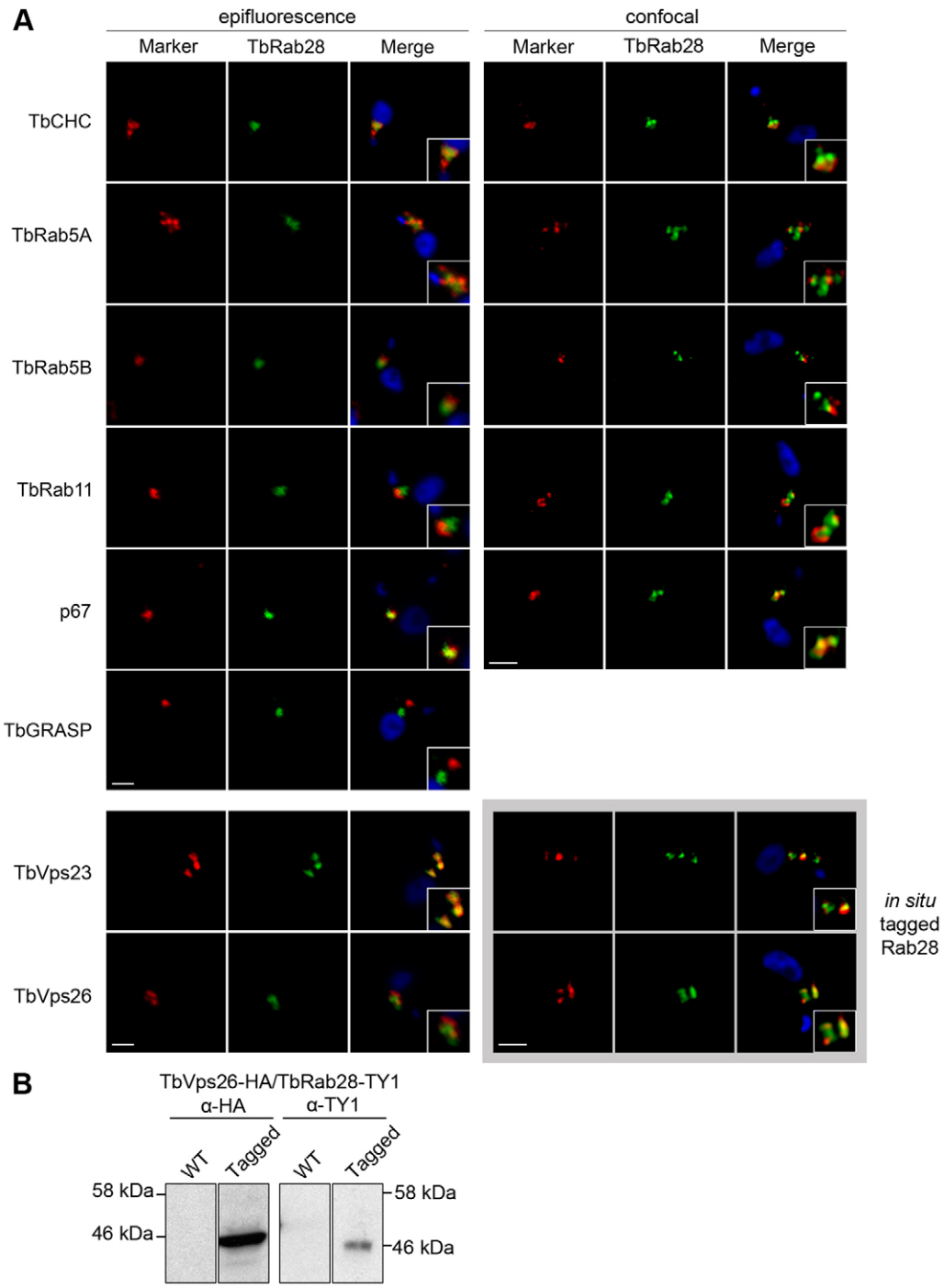


**Fig. 2. Subcellular localization of *T. brucei* Rab28.** (**A**) BSF cells expressing HA- and YFP-tagged Rab28 co-stained with endosome markers were imaged by epifluorescence and confocal microscopy. Confocal images shown are a single central Z-section of a deconvolved image stack. Rab28 is shown in green; CHC, Rab5A, ISG100 (an undefined antigen of the Rab5B compartment) (Pal et al., 2002), Rab11, GRASP and p67 are shown in red. *T. brucei* Vps23 and Vps26 were localized by dual expression of TbRab28YFP (green) and HA-tagged Vps23 or Vps26 (red). To eliminate the possibility of mislocalization due to overexpression, *T. brucei* Rab28 was in situ tagged with a TY1 epitope and co-expressed with HA-tagged Vps23 and Vps26 (gray box). Inserts are electronic magnifications of regions of interest. Scale bars: 2 μm. (**B**) Western blot of total protein samples ($10^7$ cells per lane) from in situ tagged Rab28TY1/Vps26HA dual expression cells. Western blotting was performed using anti-HA and anti-TY1 antibodies.

induced cells had decreased by 50%, and remained at this level for the duration of the experiment. The proliferation defect was not due to a cell cycle block, suggesting a more specific functional mechanism whereby proliferation was reduced while cell morphology remained normal (data not shown). The absence of a BigEye phenotype (Allen et al., 2003; Hall et al., 2004) caused by engorgement of the flagellar pocket due to blockade in endocytic membrane uptake, suggests that *T. brucei* Rab28 does not function in bulk uptake of membrane or early endocytosis, consistent with the absence of Rab28 from early endosomal compartments. Rab28 is scored as non-essential in BSF cells using a whole genome scan approach but, interestingly, does appear to be essential in PCFs (Alsford et al., 2011).

As 90% of the total surface glycoprotein in trypanosomes is the variant surface glycoprotein (VSG), and hence VSG is the overwhelming mannose-containing surface macromolecule, uptake of the mannose-binding lectin concanavalin A (ConA) mainly reports on VSG endocytosis (Overath et al., 1994; Cross, 1996; Mehlert et al., 2002; Allen et al., 2003). To address a possible role for Rab28 in surface protein endocytosis, we monitored ConA accumulation in *T. brucei* Rab28$^{RNAi}$ cells. Quantitative fluorescence microscopy clearly showed that

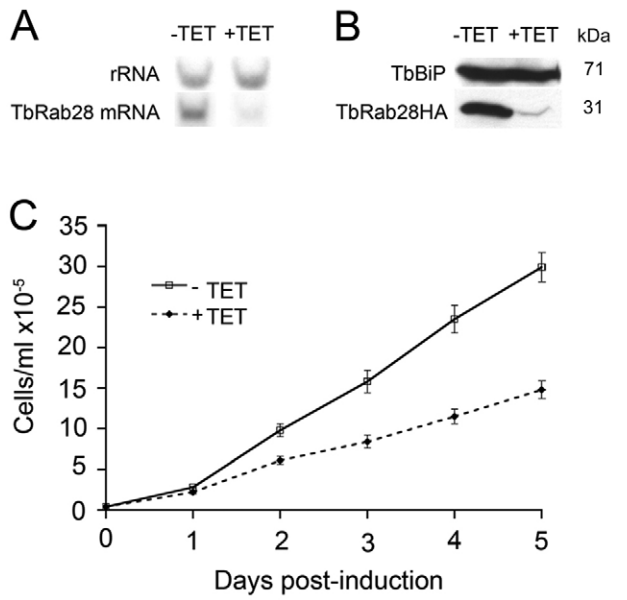


**Fig. 3. Effect of RNAi against *T. brucei* Rab28.** (**A**) Validation of *T. brucei* Rab28 knockdown by northern blot. RNA samples were collected from parasites grown for 24 hours in the presence (+TET) or absence (−TET) of 1 μg/ml tetracycline, and *Rab28* mRNA levels assessed by northern blotting. The blot was re-probed for rRNA as a loading control. (**B**) Representative western blot of total protein samples ($10^7$ cells per lane) from *T. brucei* Rab28HA$^{RNAi}$ cells. TbRab28HA was expressed in a *T. brucei* Rab28$^{RNAi}$ mutant background, and parasites induced or not induced for a total of 24 hours. Western blotting was performed using anti-HA antibodies revealing efficient knockdown of Rab28 at the protein level. BiP levels remain unchanged during Rab28 knockdown. Approximate molecular weights, as inferred using co-electrophoresed molecular weight markers, are shown. (**C**) Cumulative proliferation curves for *T. brucei* Rab28$^{RNAi}$ cells under non-induced (solid lines) and induced (dashed line) conditions. Each day, parasite numbers were determined and cultures maintained in mid-logarithmic phase by dilution. Readings are the cumulative mean cell number; error bars are s.e.m. over triplicate inductions.

accumulation of fluorescein isothiocyanate (FITC)–ConA was compromised in *T. brucei* Rab28 knockdown cells (Fig. 4A). To verify this observation, cells were co-stained with antibodies to p67. ConA normally accumulates in the lysosome of trypanosomes (Brickman et al., 1995), but RNAi against *T. brucei* Rab28 prevented delivery of ConA to the lysosome in 80% of cells, resulting in retention in a pre-lysosomal compartment (Fig. 4B,C). These data suggest defective endocytic transport as a consequence of Rab28 suppression and a failure to deliver cargo to the lysosome.

Because ConA is not a physiologically relevant ligand, and the lectin essentially reports bulk glycoprotein flow (Overath and Engstler, 2004), we selected the transferrin receptor (which in trypanosomes is a GPI-anchored heterodimer) to examine receptor-mediated endocytosis (Steverding et al., 1995). Accumulation of Alexa-Fluor-633-labelled transferrin, measured using fluorescence activated cell sorting (FACS), revealed a dramatic 67% decrease in transferrin accumulation in *T. brucei* Rab28$^{RNAi}$ cells (Fig. 4D), suggesting a requirement for Rab28 in receptor-mediated uptake and indicating a general impact of Rab28 depletion on endocytosis.

Unlike the extensive recycling of transferrin observed in mammalian cells, transferrin is extensively degraded within the trypanosomal endosomal system by *T. brucei* catB, a cathepsin B-related protease (Mackey et al., 2004; Grab et al., 1992). The resulting peptide digestion products are exported via a Rab11-dependent recycling pathway (Steverding et al., 1995; Pal et al., 2003). To investigate whether there is a role for *T. brucei* Rab28 in this process, loss of accumulated Alexa-Fluor-633–transferrin was followed in knockdown cells. The fluorophore survives endosomal (catB) exposure, making this a suitable method for analyzing the recycling pathway (Pal et al., 2003). Fluorescence decay kinetics were essentially identical in control and Rab28 knockdown cells (Fig. 4E), suggesting that *T. brucei* Rab28 does not play a major role in re-export of transferrin-derived peptides.

### *T. brucei* Rab28 mediates sensitivity to trypanosome lytic factor

*T. brucei* are sensitive to trypanosome lytic factor (TLF), an innate immune factor in human serum (Hager et al., 1994). TLF is a component of the HDL fraction and manifests trypanolytic activity at the lysosome (Perez-Morga et al., 2005; Raper et al., 2001; Pays et al., 2006). TLF undergoes receptor-mediated endocytosis, traversing the flagellar pocket, early endosomes and late endosome prior to reaching the lysosome (Vanhollebeke et al., 2008). We examined TLF sensitivity after *T. brucei* Rab28 RNAi to analyze terminal endocytic events and lysosomal delivery.

Cells were incubated in varying concentrations of normal human serum. Silencing *T. brucei* Rab28 significantly decreased the sensitivity of trypanosomes to TLF. For example, after 4.5 hours in 10% human serum, cell survival in Rab28$^{RNAi}$ cells was increased by 41% ($P<0.005$) compared with control cells (Fig. 4F). The effect was specific to *T. brucei* Rab28$^{RNAi}$ cells, as silencing of a second late endosomal protein, Vps23 (Leung et al., 2008) failed to elicit this effect (Fig. 4G). These data suggest that depletion of Rab28 significantly impairs trafficking of TLF to the lysosome, consistent with the defect in ConA lysosomal delivery.

### *T. brucei* Rab28 is required for turnover of invariant surface glycoproteins

The data above indicate a role in late endocytosis for *T. brucei* Rab28, consistent with partial colocalization with Vps23, a component of ESCRT I (Babst et al., 2000). A possible role for *T. brucei* Rab28 in turnover of internalized surface proteins was examined. Invariant surface glycoproteins 65 and 75 (ISG65 and ISG75) are abundant type I cell surface *trans*-membrane proteins possessing multiple cytoplasmic lysine residues and undergo ubiquitin-dependent degradation (Chung et al., 2004; Leung et al., 2011).

ISG75 turnover was examined in *T. brucei* Rab28$^{RNAi}$ cells following cycloheximide treatment. After 4 hours, ISG75 levels are reduced by 50% in non-induced cells, but in Rab28-depleted cells, ISG75 levels are reduced less than 10% (Fig. 5A). This suggests that *T. brucei* Rab28$^{RNAi}$ cells cannot efficiently turnover ISG75 and that Rab28 has a possible role in sorting at the late endosome, where ubiquitylated proteins are presumably targeted to the lysosome. To confirm this, the levels of intracellular ISG75 were monitored by immunofluorescence. A highly significant 50% increase ($P<0.0001$) in intracellular ISG75 levels was observed in *T. brucei* Rab28$^{RNAi}$ cells relative

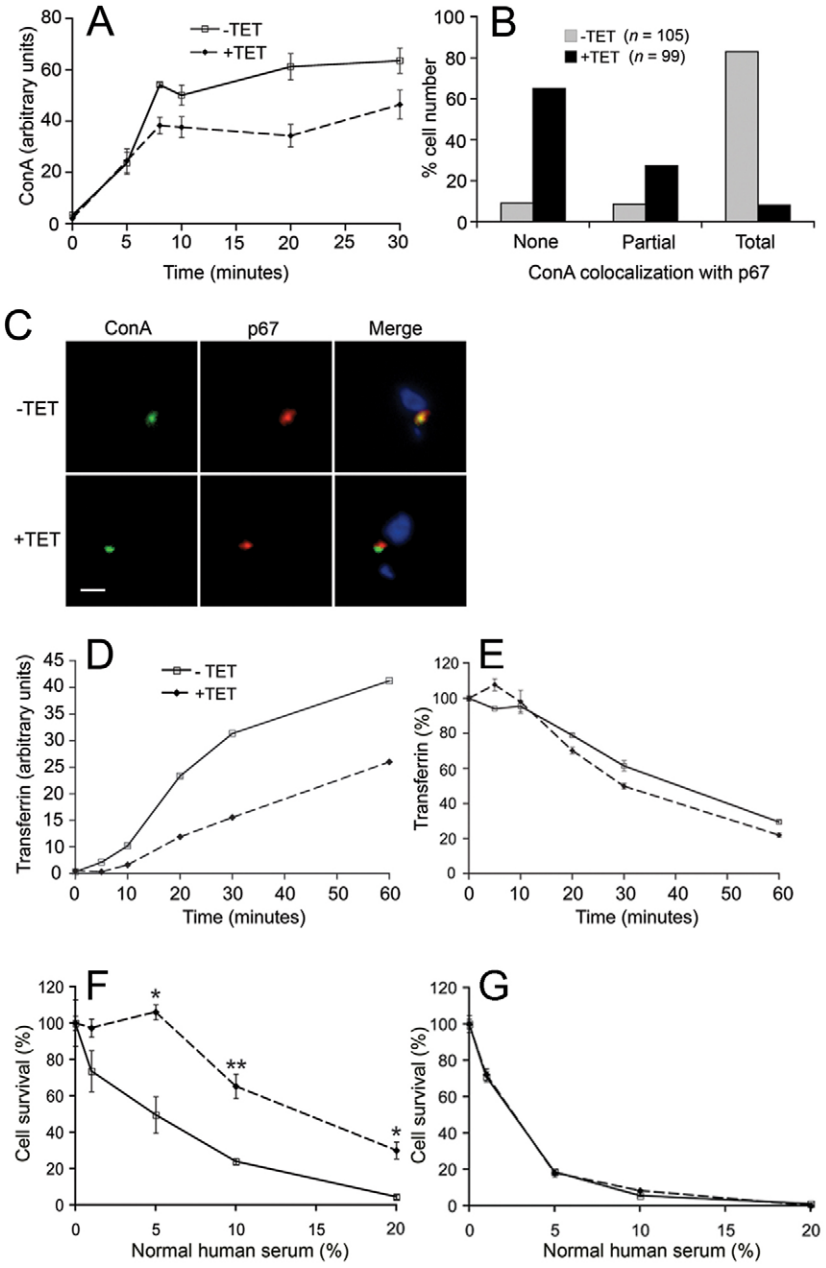


**Fig. 4. *T. brucei* Rab28 depletion effects endocytosis.** (**A**) ConA accumulation in Rab28-depleted cells. *T. brucei* Rab28$^{RNAi}$ cells were incubated with FITC-conjugated ConA at 37℃. ConA fluorescence was measured using Metamorph ($n$=20). The experiment was repeated by FACS in triplicate and generated highly similar results. (**B**) ConA and p67 colocalization in control (−TET) and induced (+TET) *T. brucei* Rab28$^{RNAi}$ cells. Cells were exposed to FITC-conjugated-ConA for 30 minutes at 37℃ and co-stained for p67 (red). ConA/p67 colocalization frequency ($n$=200) was assessed using Metamorph. (**C**) Representative images of *T. brucei* Rab28$^{RNAi}$ cells. After 30 minutes, ConA substantially colocalized with p67 in control cells, but most ConA and p67 was confined to separate structures in RNAi cells. Scale bar: 2 μm. (**D**) Transferrin uptake in *T. brucei* Rab28$^{RNAi}$ cells ($n$=3). (**E**) Cells were allowed to accumulate Alexa-Fluor-633–transferrin and then chased for the indicated times. Fluorescence is expressed relative to cells at time zero (100%) ($n$=3). (**F**) Survival of *T. brucei* Rab28$^{RNAi}$ cells in varying amounts of human serum. Values are the mean of triplicate inductions relative to survival of non-induced cells in 20% FCS (100%). (**G**) Survival of *T. brucei* Vps23$^{RNAi}$ cells in varying amounts of human serum. Values are the mean of triplicate inductions relative to survival of non-induced cells in 20% FCS (100%). Error bars show s.e.m. and are sometimes obscured by symbols. *$P$<0.05, **$P$<0.005.

to non-induced cells, correlating with decreased ISG75 turnover (Fig. 5B,E). Importantly, at steady state, total protein levels of ISG75 were unchanged in Rab28-depleted cells, ruling out a general increase to ISG75 levels (Fig. 5C). Similarly, increased intracellular levels of ISG65 were observed in induced cells compared with non-induced cells, with an even more pronounced effect than ISG75 (Fig. 5D,E). We were unable to detect any significant change in ISG65 or ISG75 levels on the surface of the cells by FACS analysis, but as we did not have an accurate estimate of relative internal and external pool sizes, this might reflect changes in a comparatively small intracellular pool (data not shown). Previous analysis demonstrated that, in common with higher eukaryotes, turnover of ubiquitylated proteins is dependent on the ESCRT pathway (Chung et al., 2008), so we propose that the increase in intracellular ISG65 and ISG75 following Rab28 depletion is due to failure to progress to the lysosome, similar to the effects of Rab28 RNAi on both ConA and TLF.

### *T. brucei* Rab28$^{RNAi}$ cells exhibit morphological defects in recycling endosomes and the Golgi complex

To further delineate pathways requiring Rab28 expression, markers of intracellular compartments were monitored using both western blotting and IFA, to examine both expression levels and the location of the marker proteins. No obvious changes in distribution or total protein levels of clathrin heavy chain (CHC) or Rab5A were observed in *T. brucei* Rab28$^{RNAi}$ cells (Fig. 6A,C), which suggests that Rab28 is not directly involved in formation or distribution of clathrin-coated vesicles or early endosomes, and is consistent with the localization of Rab28.

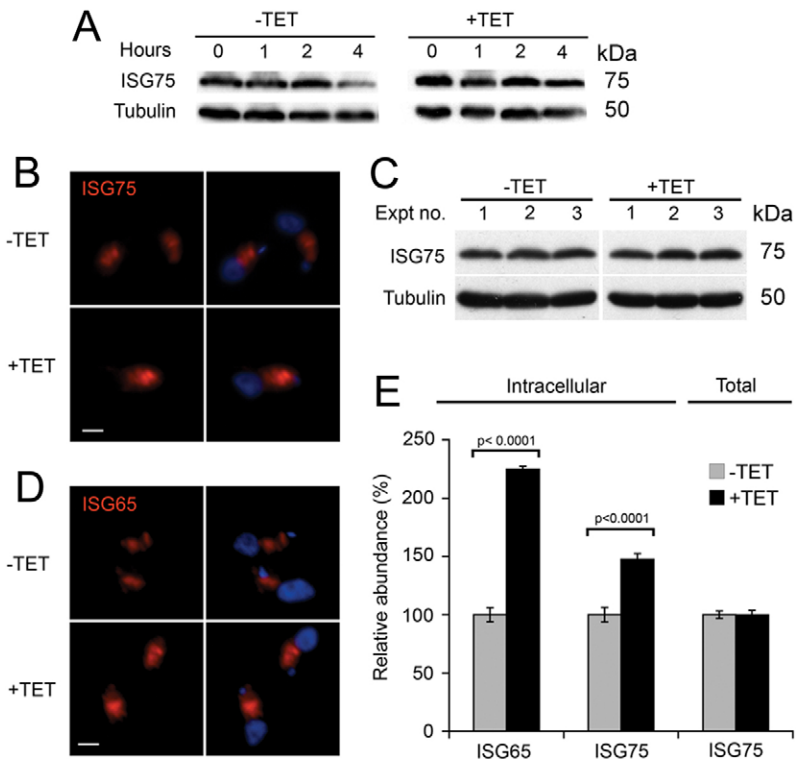


**Fig. 5. *T. brucei* Rab28 is required for ISG turnover.** (**A**) Western blot of ISG75 turnover in control (−TET) and *T. brucei* Rab28$^{RNAi}$ cells after 36 hours of induction (+TET). β-tubulin was used as a loading control due to its long half-life. Representative image from three replicate inductions. Scale bar: 2 µm. (**B**) Induced and non-induced *T. brucei* Rab28$^{RNAi}$ cells were stained with polyclonal antibodies to ISG75 (red). Representative images captured under identical exposure conditions. (**C**) Western blot of total ISG75 protein levels in *T. brucei* Rab28$^{RNAi}$ cells. Three biological replicates are shown. (**D**) *T. brucei* Rab28$^{RNAi}$ cells stained with polyclonal antibodies to ISG65. Representative images captured under identical exposure conditions. (**E**) Quantification of intracellular immunofluorescence (left) and total protein abundance (right) from analyses in B, C and D. Mean intracellular immunofluorescence in induced cells ($n$=30) was normalized to non-induced cells (ISG65 $n$=48; ISG75 $n$=28). Total protein levels were quantified by densitometry, normalized to β-tubulin in non-induced cells (100%). Significance assessed with Student's $t$-test.

However, structural alterations to recycling compartments marked by Rab11 were observed in *T. brucei* Rab28$^{RNAi}$ cells. A gradual expansion of Rab11 staining was seen over 4 days, but this was not accompanied by an increase to Rab11 protein levels (Fig. 6A,C). Expansion of Rab11 localization required 4 days to become apparent but Rab28 was silenced within 24 hours, which suggests that progressive disruption to recycling endosomes is probably a secondary effect, possibly as a consequence of the pre-lysosomal blockade to traffic and/or re-routing of endocytic cargo through the recycling pathway. Additionally, disordered compartments might result from defective targeting of components essential for maintaining structural integrity of recycling endosomes.

Surprisingly, Rab28 knockdown had dramatic effects on Golgi complex morphology (Fig. 6A). Silencing Rab28 resulted in fragmentation of Golgi membranes as monitored by GRASP immunoreactivity. Control cells in G1 possess a maximum of three GRASP spots, whereas 15% of *T. brucei* Rab28$^{RNAi}$ cells displayed more than five GRASP spots after 24 hours. After 48 hours of RNAi, complete dispersal of the Golgi complex was observed in 30% of *T. brucei* Rab28$^{RNAi}$ cells (Fig. 6B). This observation was verified with a second Golgi complex marker, Rab1 (Dhir et al., 2004). In *T. brucei* Rab28$^{RNAi}$ cells, Rab1-positive membranes also expanded, providing further evidence that Rab28 expression is required to retain Golgi architecture, which suggests that *T. brucei* Rab28 participates in retrograde trafficking from late endosomes to the Golgi complex. Importantly, perturbation of Golgi architecture occurred with kinetics more similar to Rab28 knockdown, and is therefore a more direct consequence of Rab28 loss than alterations in recycling endosomes. Clearly, disruption of the Golgi complex will impact multiple trafficking pathways and possibly accounts for the expansion of Rab11 endosomes.

Most intracellular VSG is associated with the Golgi complex and the endoplasmic reticulum (ER) (Webster and Grab, 1988). In permeabilized cells, residual surface staining of VSG was seen, together with ER and Golgi intracellular pools. However, in Rab28-depleted cells, intracellular VSG appeared diffuse compared with control cells (Fig. 6A), which is also consistent with Golgi disruption. These data suggest that a focus of intracellular VSG (i.e. the Golgi complex) became dispersed over time.

Finally, a mild perturbation in lysosome morphology was observed in *T. brucei* Rab28$^{RNAi}$ cells, with expansion of p67 staining (Fig. 6A). This effect was moderate because most (~70%) *T. brucei* Rab28$^{RNAi}$ cells contained morphologically normal lysosomes, and indicates that, although p67 is faithfully targeted in cells depleted of Rab28, targeting of other, so far unidentified lysosomal structural components might be affected.

### Golgi complex ultrastructure is perturbed by *T. brucei* Rab28 silencing

To further examine the effect of *T. brucei* Rab28 RNAi on subcellular structures we analyzed cells by transmission electron microscopy (TEM). After 36 hours of RNAi against Rab28, the majority of induced cells lacked discernible stacked Golgi complexes (Fig. 7C,D). Where present, membranes in the region of the cell normally containing the Golgi complex exhibited anomalous cisternal structures (Fig. 7B). Significantly, a detectable Golgi was completely absent at 96 hours post-induction. In 15 sections from unperturbed cells we found five stacks (i.e. in 33% of sections) but we were unable to observe a single stacked Golgi complex in over 50 sections from the *T. brucei* Rab28$^{RNAi}$ cells (not shown and Fig. 7E). Furthermore, we infrequently detected structures with a high proportion of intralumenal vesicles (Fig. 7E), as previously been reported when

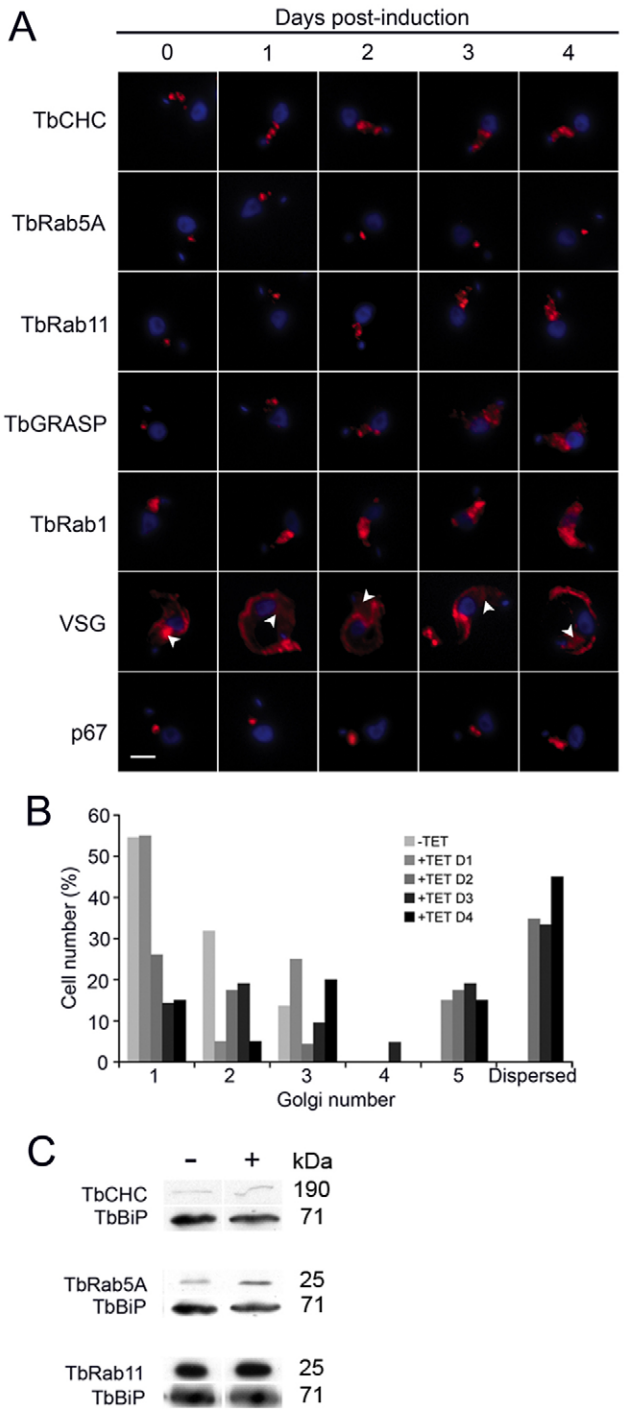


**Fig. 6. Analysis of membrane trafficking compartments in *T. brucei* Rab28-depleted cells.** (**A**) *T. brucei* Rab28$^{RNAi}$ cells were induced and then stained with antibodies against various cellular components. Each image is representative of 10. Arrowheads mark intracellular VSG. (**B**) Quantification of GRASP-positive puncta in non-induced and induced *T. brucei* Rab28$^{RNAi}$ cells ($n$=20). Designation of more than five spots was scored as 'Dispersed'. D, days post-induction. (**C**) Western blots for CHC, Rab5A and Rab11 at steady state in *T. brucei* Rab28$^{RNAi}$ whole cell lysates. BiP was used as loading control. Data are representative of at least two determinations. Scale bar: 2 μm.

AP-1 was silenced in trypanosomes, which might correspond to multivesicular bodies or other stress-induced structures (Allen et al., 2007). We also observed the appearance of highly vesiculated structures in close proximity to the flagellar pocket; these structures might represent residual material derived from the Golgi complex, post-Golgi transport intermediates and/or endosomal structures (Fig. 7E). By contrast, the subpellicular array of microtubules, flagellum attachment zone and flagellum all retained normal architecture, which signifies a specific defect to endomembrane trafficking networks. These data are fully consistent with the effects seen at the Golgi complex and recycling endosomes observed using light microscopy.

### *T. brucei* Rab28 depletion perturbs expression of ESCRT and retromer subunits

In mammalian cells, retromer mediates trafficking from endosomes to the Golgi complex (Seaman, 2004; Arighi et al., 2004; Belenkaya et al., 2008). *T. brucei* possesses orthologues of the cargo-recognition retromer subcomplex (Vps26, Vps29 and Vps35) and one sorting nexin (Vps5), suggesting conserved function (Koumandou et al., 2011).

Vps26-associated fluorescence was reduced by 75% in *T. brucei* Rab28$^{RNAi}$ cells and was accompanied by decreased protein levels, indicating that Rab28 expression influences Vps26 protein stability and/or synthesis (Fig. 8A–C). To determine whether Rab28 acts upstream or downstream of Vps26, a *T. brucei* Vps26$^{RNAi}$ cell line expressing TbRab28HA was generated. Rab28 levels were monitored by western blot after induction of RNAi against Vps26. Rab28 levels remained unchanged in *T. brucei* Vps26$^{RNAi}$ cells, indicating that Rab28 functions upstream of Vps26 (Fig. 8H).

To further investigate involvement of Rab28 in late endosomal trafficking, the effects of Rab28 knockdown on ESCRT I were analyzed. Vps23 was undetectable by IFA in *T. brucei* Rab28$^{RNAi}$ cells (Fig. 8D), a result reflected in total protein levels in lysates, which were reduced by ~70% (Fig. 8E). To assess whether Rab28 knockdown resulted in a general impact on ESCRT I and the expression of Vps28, a second epitope-tagged ESCRT I subunit was monitored (Leung et al., 2008). A similar decrease was observed, representing an ~80% reduction in total protein levels (Fig. 8D–F). These data demonstrate that the stability of the ESCRT I complex as a whole was compromised by silencing Rab28. *T. brucei* Vps23 was silenced in cells containing TbRab28HA. Rab28 levels were unaltered in Vps23-depleted cells, suggesting that *T. brucei* Rab28 functions upstream of Vps23 (Fig. 8G). To characterize interactions between Rab28 and Vps23 and Vps26, *T. brucei* Vps23 was silenced and the HA-tagged Vps26 (TbVps26HA) levels monitored. Although some increase in Vps26 was found (Fig. 8G), Vps26 knockdown failed to elicit *in trans* effects on TbVps23HA (Fig. 8H). Hence, there is no evidence for *in trans* suppression between *T. brucei* Vps26 and Vps23 expression, suggesting that these effects are mediated via loss of Rab28.

## Discussion

Rab proteins regulate recognition, fusion and fission events in membrane transport. In endocytosis, maturation of early into late endosomes is marked by Rab5 to Rab7 conversion (Rink et al., 2005) and a switch in the repertoire of Rab effectors and other proteins on the endosomal membrane in a coordinated process. Overall, however, the endocytic system is very complex and involves additional Rab proteins, including Rab4, Rab11

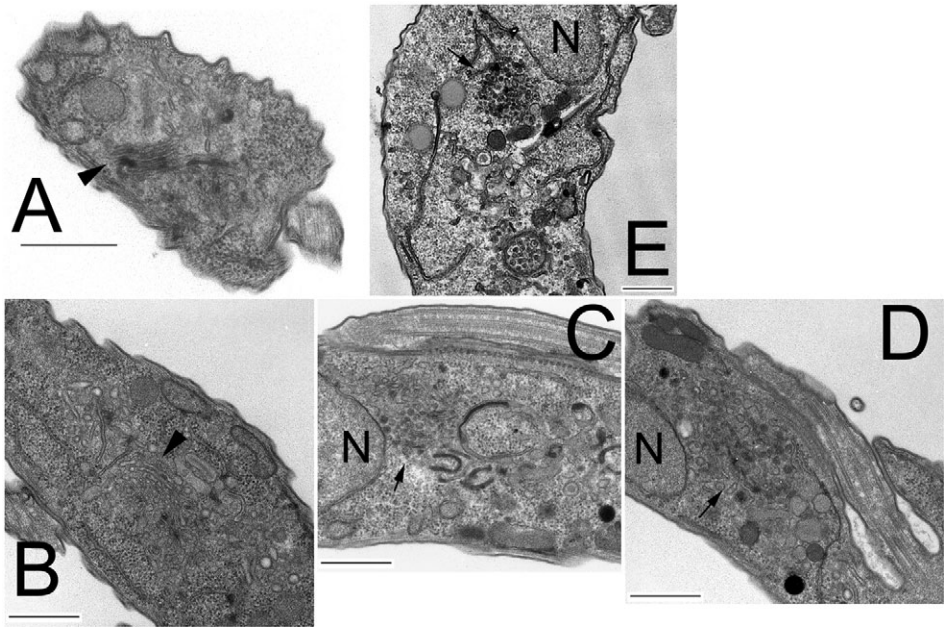


**Fig. 7. Ultrastructure of *T. brucei* Rab28$^{RNAi}$ cells.** (**A**) Uninduced *T. brucei* Rab28$^{RNAi}$ cells. (**B**–**D**) Induced (36 hours) *T. brucei* Rab28$^{RNAi}$ cells. (**E**) Induced (96 hours) *T. brucei* Rab28$^{RNAi}$ cells. Arrowheads indicate stacked Golgi and Golgi-like cistern; arrows, vesicular clusters in the cell region normally occupied by the Golgi complex; N, nucleus. Scale bars: 500 nm (A); 1 µm (B–E).

and Rab21. We have analyzed the function of trypanosome Rab28, which appears to also mediate endocytic traffic, including endocytosis of transferrin, turnover of *trans*-membrane domain endocytic cargo glycoproteins and lysosomal delivery. Furthermore, although *T. brucei* Rab28 was required for proliferation, knockdown did not perturb cell cycle progression nor result in a global blockade of membrane uptake from the trypanosome endocytic organelle, the flagellar pocket. Together with partial colocalization with Vps23, we suggest that *T. brucei* Rab28 predominantly localizes to late endocytic compartments.

Knockdown of *T. brucei* Rab28 resulted in a pre-lysosomal transport block, implicating Rab28 in sorting material prior to lysosomal delivery. An *in trans* decrease in expression levels of ESCRT I (Vps23 and Vps28) and retromer complex (Vps26) proteins on Rab28 knockdown suggests a functional connection between Rab28, ESCRT and retromer. The effects on ESCRT are fully consistent with the observed partial protection of ISG65 and ISG75, as both require ubiquitylation for turnover and, hence, are probably sorted by the ESCRT system (Chung et al., 2008; Leung et al., 2011). The effects on the Rab11 recycling compartment suggest increased cycling of cargo between endosomes, as reported upon silencing of Vps26 and Vps23 in mammalian cells (Seaman, 2004; Razi and Futter, 2006; Raiborg et al., 2008). The partial protection of ISG75 is probably due to incomplete silencing of *T. brucei* Rab28, as found earlier for *T. brucei* Vps23 (Leung et al., 2008), although we cannot exclude Rab28-independent pathways. Significantly, *T. brucei* Rab28 probably functions upstream of Vps23 and Vps26, as knockdowns of the latter did not affect Rab28 expression. The clear complexity of trafficking within this region of the trypanosome endomembrane system suggests that analysis of the roles that Rab5 and Rab11 play in ISG transport will be highly informative, especially as our understanding of these pathways has advanced somewhat since the original descriptions of these pathways (Field and Carrington 2009).

Disruption of Golgi complex morphology by Rab28 knockdown was unexpected because Rab28 does not localize at Golgi membranes, but a similar kinetic profile for disruption of Rab1, Rab11 and GRASP location argues for a fairly comprehensive impact affecting both the *cis* and *trans* faces as well as the stack itself. Disruption of sphingolipid biosynthesis through inhibition of serine palmitoyltransferase has a similar effect on the Golgi complex, but the effect is relatively mild (Fridberg et al., 2008). However, disruption of Golgi morphology upon depletion of *T. brucei* Rab28 parallels Vps26 knockdown in mammalian cells and trypanosomes (Seaman, 2004; Koumandou et al., 2011). The absence of conventional retromer cargo from trypanosomes means that direct investigation of retromer function is difficult, but the complex probably mediates similar functions in both systems (Koumandou et al., 2011). Gross morphological aberrations at the Golgi complex potentially result through depletion of SNAREs or other factors required for correct homotypic fusion due to defective retrieval from late endosomes, i.e. a ‘traffic jam’.

Although mechanisms coordinating retrograde transport with endosomal maturation are well understood, precisely how the functions of the sorting complexes involved in retrograde and anterograde transport are integrated remains elusive. Specifically, both retromer and ESCRT participate in transport at late endosomal compartments, but their very distinct functions necessitate coordination. *T. brucei* Rab28 could be required for maintaining structural boundaries at endosomes or for correct assembly of ESCRT and/or retromer complexes, and potentially in controlling turnover of ubiquitylated cargo, which is probably a major route for degradation of surface proteins in trypanosomes (Leung et al., 2011). Depletion of *T. brucei* Rab28 resulted in extensive morphological defects, suggesting that Rab28 is required to maintain endosome structure. Direct interactions between *T. brucei* Vps23 and Rab28 were not detected by co-immunoprecipitation (data not shown), but it is possible that interaction is mediated via Rab28 effector proteins for example

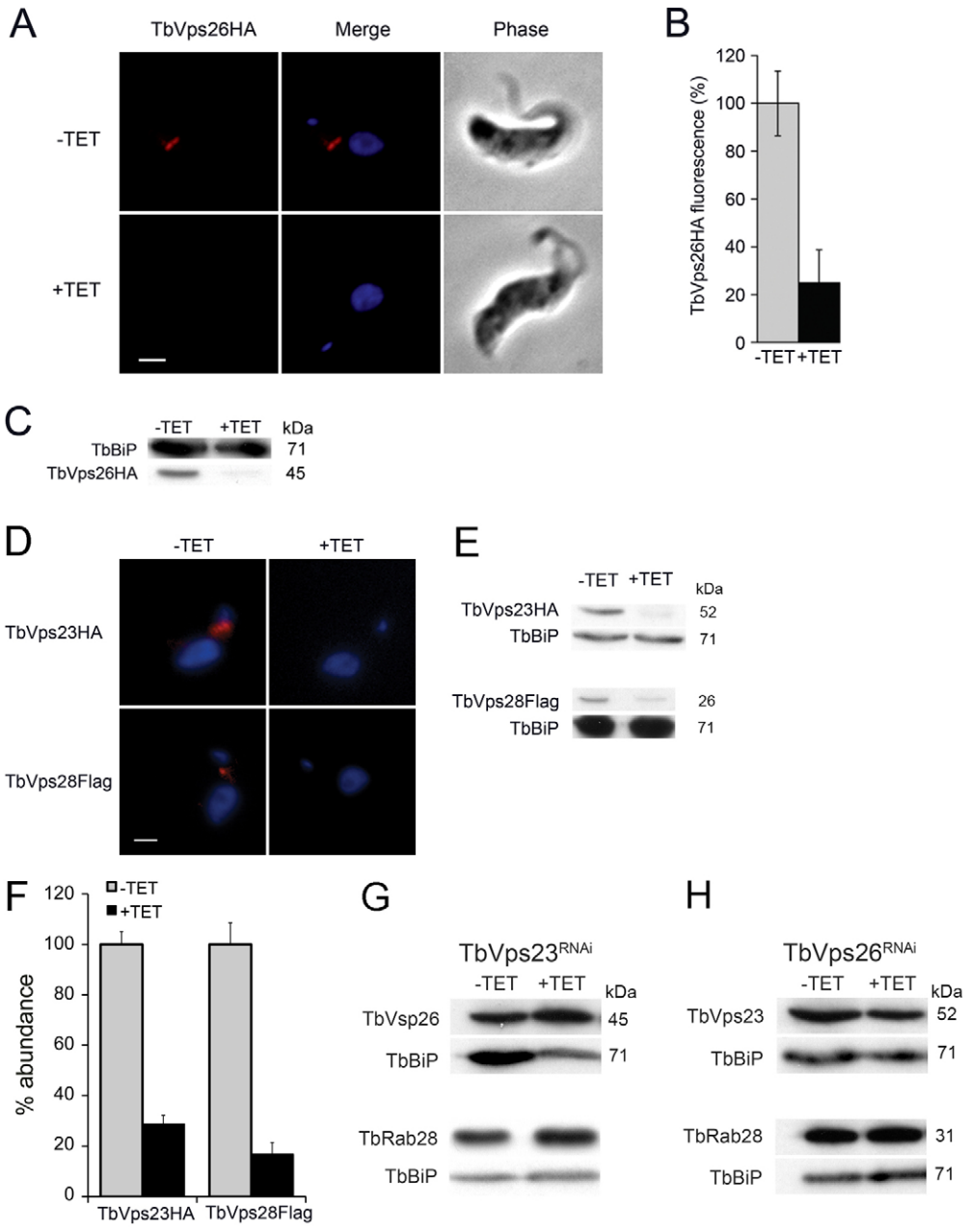


**Fig. 8. Analysis of Vps26 and ESCRT complex in *T. brucei* Rab28$^{RNAi}$ cells.** (**A**) IFA on control (–TET) and induced (+TET) *T. brucei* Rab28$^{RNAi}$ cells expressing HA-tagged Vps26. Cells were stained with anti-HA to visualize TbVps26HA (red). (**B**) Quantification of TbVps26HA immunofluorescence levels in induced cells (+TET, $n$=54) normalized to control cells ($n$=48). Error bars indicate s.e.m. of triplicate inductions. (**C**) Representative western blot from triplicate inductions of TbVps26HA protein in *T. brucei* Rab28$^{RNAi}$ non-induced and induced whole cell lysates. (**D**) IFA on non-induced and induced *T. brucei* Rab28$^{RNAi}$ cells expressing TbVps23HA or TbVps28FLAG. Cells were stained with anti-HA or anti-FLAG antibodies (red). (**E**) Representative western blot from triplicate inductions of TbVps23HA and TbVps28FLAG expression in whole cell lysates from non-induced and induced cells expressing TbVps23HA or TbVps28FLAG. (**F**) Quantification of TbVps23HA and TbVps28FLAG expression in *T. brucei* Rab28$^{RNAi}$ non-induced and induced cells. Mean values were obtained by densitometry of blots and have been normalized to expression in non-induced cells (100%). Error bars indicate the s.e.m. from triplicate inductions. (**G**) Representative ($n$=3) western blot of non-induced and 24-hour-induced *T. brucei* Vps23$^{RNAi}$ cells expressing either HA-tagged Vps26 or Rab28. Loading was $10^7$ cell equivalents per lane, verified using BiP. (**H**) Representative ($n$=3) western blot on non-induced and 24-hour-induced *T. brucei* Vps26$^{RNAi}$ cells expressing either HA-tagged Vps23 or Rab28. Loading as for G. Scale bars: 2 μm.

and that Rab28 is itself controlled by the relevant GAP and GEF proteins. Furthermore, ESCRT 0 recruits ESCRT I in mammalian cells (Bache et al., 2003; Katzmann et al., 2003), but ESCRT 0 is absent from most organisms and the primary mechanism of ESCRT recruitment in trypanosomes is unclear (Leung et al., 2008). Significantly, ESCRT 0 depletion in mammalian cells failed to abolish epidermal growth factor receptor degradation and only inhibits Vps23 membrane association by ~50%, which suggests the presence of alternative recruitment mechanisms (Razi and Futter, 2006; Bache et al., 2003; Katzmann et al., 2003).

Clearly, species retaining Rab28 must have distinct mechanisms for coordinating ESCRT and retromer function compared with Rab28-deficient species. Importantly, trypanosome Rab28 is 80% identical to human Rab28 in the switch and interswitch regions, and these regions are key in determining effector interactions (Delprato and Lambright, 2007; Eathiraj et al., 2005; Merithew et al., 2001). Together with observations that orthologues generally retain similar functions across evolution (Brighouse et al., 2010), this suggests that *T. brucei* Rab28 is probably functionally homologous to *H. sapiens* RAB28 and provides a mechanism allowing sorting and subsequent degradation of ubiquitylated cargo in the absence of the ESCRT 0 subunit, Hrs (Razi and Futter, 2006; Bache et al., 2003; Hammond et al., 2003). Moreover, increased autophagosome frequency is observed when ESCRT complexes are inactivated, suggesting that ESCRT is involved in autophagosome–lysosome fusion events (Doyotte et al., 2005; Filimonenko et al., 2007; Lee et al., 2007). Silencing *H. sapiens* RAB28 dramatically inhibits autophagosome formation (Nicole

McKnight and Sharon Tooze, Cancer Research UK, London, personal communication), also implicating *H. sapiens* RAB28 in generation of autophagosomes, possibly through regulation of ESCRT function. ESCRT, retromer and autophagocytosis are essential for cellular homeostasis, and malfunctions in these systems contribute to multiple pathologies (Hu et al., 2006; Tanida et al., 2005; Kirschbaum and Yarden, 2000; Vaccari and Bilder, 2005; Moberg et al., 2005; Thompson et al., 2005). There is a highly significant correlation between familial breast cancer and a single-nucleotide polymorphism directly upstream of *H. sapiens* RAB28 (Yang et al., 2008), which is consistent with a role for Rab28 in sorting of ubiquitylated proteins and, specifically, mitogenic receptors.

## Materials and Methods

### Cell lines

Bloodstream form (BSF) and procyclic form (PCF) Lister 427 strains were maintained in HMI-9 and SDM79 medium, respectively, as described (Field and Field, 1997). Single marker BSF (SMB) cells (Wirtz et al., 1999) were maintained with 2.5 μg/ml neomycin. Cells in exponential growth, $<1\times10^6$/ml and $3–8\times10^6$ cells/ml for BSF and PCF cells, respectively, were used for all experiments.

### Generation of transgenic parasites

A 581 bp fragment from position 109–690 of the *T. brucei* Rab28 ORF (Tb927.6.3040) was amplified using primers 5′-GCGACAGTTCAGACTC-AGAAAA-3′ and 5′-CACTGCGCATTTACCCTTCT-3′ (Redmond et al., 2003) and cloned into p2T7$^{TABlue}$. An AMAXA Nucleofector II was used to transfect SMB cells with *Not*I-digested plasmid. Clones were selected and maintained in the presence of 5 μg/ml hygromycin and 2.5 μg/ml geneticin. For ectopic expression *T. brucei* Rab28 was amplified from genomic DNA using primers 5′-CCAGAAGCTTCTAGTAGCGACAGTTCAGACTCAG-3′ and 5′-GCATGGA-TCCCTACATCACTGCGCATTTAC-3′ and cloned into pHD1034 (Quijada et al., 2002) or pXS519 (Hall et al., 2004) containing N-terminal HA or YFP for expression in BSF and PCF cells, respectively. BSF cells were transfected with 5 μg linearized pHD1034-*T. brucei* Rab28 and clones maintained in 2.5 μg/ml geneticin and 0.2 μg/ml puromycin. PCFs were transformed as described (Hall et al., 2004). Plasmids allowing ectopic expression of *T. brucei* Vps23HA, Vps28FLAG and Vps26HA were as described (Leung et al., 2008; Koumandou et al., 2011).

### N-terminal epitope-tagging at the endogenous locus

To express *T. brucei* Rab28 at the endogenous locus, the 5′-end ORF was generated by PCR using the following primers: Rab28 GTag_F2 (5′-CTCAAGCTTTGATGAGTAGCGACAGTTCAGACTC-3′) and Rab28 GTag_R3 (5′-CGCGATATCGTCGCTGCCAACTGCGTGAAG-3′). The PCR product was first cloned into pGEM-T Easy plasmid vector (Promega) and subsequently subcloned with *Hin*dIII and *Eco*RV into plasmid vector p3077 (a gift from Mark Carrington, University of Cambridge, UK) (Kelly et al., 2007) that generates an N-terminal 4× TY1 epitope-tagged fusion protein. Plasmid was linearized using the unique *Sph*I site within the 5′-end ORF prior to transfection into cells. For immunofluorescence assay, detection was achieved using BB2 monoclonal antibody (a gift from Keith Gull, University of Oxford, UK) at 1:10 dilution and at 1:50 dilution for western blot analysis.

### Assessment of RNAi

RNAi was induced with 1 μg/ml TET. Silencing of *T. brucei* Rab28 was monitored by northern and western blot. BSF proliferation was monitored in triplicate by inoculating $1\times10^4$ cells/ml daily in fresh medium. Cell densities were measured with a Coulter Z1 Counter (Beckman). All assays were performed at 36 hours unless otherwise stated.

### Generation of anti-Rab28 antibodies

The *T. brucei* Rab28 ORF, without the prenylation motif, was amplified from *T. brucei* genomic DNA using primers 5′-CCTAGGATCCCCCGACAGTTC-AGACTCAGAAAAAAGG-3′ and 5′-CCTAGAATTCTTCCAAATTTAGCGC-ATCTTCAGG-3′ and ligated in-frame with GST into pGEX6p2 and transformed into BL21(DE3) *Escherichia coli*. GST::*T. brucei* Rab28 was expression-induced with 0.5 mM isopropyl β-D-thiogalactoside (IPTG). Recombinant protein was affinity-purified on glutathione Sepharose-4B (GE Healthcare). Purity of isolated GST::*T. brucei* Rab28 was estimated at ≥95% by SDS-PAGE and Coomassie Blue staining. Antiserum was raised in rabbits against the full-length fusion protein, immunizing four times with a total of 2 mg protein in Freund's complete adjuvant (Covalab). GST::*T. brucei* Rab28 was coupled to CNBr–Sepharose 4B (Sigma) for affinity purification.

### Quantitative real time PCR

$10^8$ BSF and $5\times10^7$ PCF cells were harvested at 4℃ and RNA was extracted using RNeasy (Qiagen). Complementary DNA was generated from 2 μg RNA using SuperscriptTM II RNase H reverse transcriptase (Invitrogen). qRT-PCR was performed using iQ-SYBRGreen Supermix on a Mini Opticon (BioRad). β-tubulin, expressed at similar levels in BSF and PCF cells (Diehl et al., 2002) was used to normalize. qRT primers were Rab28 forward, 5′-GCGACAGTTC-AGACTCAGAAAA-3′; Rab28 reverse, 5′-CACTGCGCATTTACCCTTCT-3′; β-tubulin forward, 5′-CAAGATGGCTGTCACCTTCA-3′; and β-tubulin reverse, 5′-GCCAGTGTACCAGTGCAAGA-3′.

### Northern blotting

Northern blotting was carried out using standard procedures. RNA was extracted from $10^8$ cells, and 3.5 μg RNA separated by gel electrophoresis prior to transfer to N-Hybond membrane. *T. brucei* Rab28 and ribosomal RNA (rRNA)-specific probes were labelled with [α-$^{32}$P]dCTP (3000 Ci/mmol) and quantified by phosphorimaging.

### Western immunoblotting

Cells were harvested, washed twice in ice-cold PBS and heated for 5 minutes at 94℃ in 2× SDS-PAGE loading buffer. $10^7$ cells per lane were resolved on 12.5% SDS–polyacrylamide gels. Proteins were electrophoretically transferred onto polyvinylidene fluoride (PVDF) membranes (Millipore), blocked and processed following standard procedures. Polyclonal rabbit anti-*T. brucei* Rab28 was used at 1:500, polyclonal rabbit anti-*T brucei* BiP serum (kind gift of James D. Bangs, University of Winsconsin, WI) 1:10,000, polyclonal rabbit anti-ISG65 serum 1:5000, polyclonal rabbit anti-ISG75 serum 1:5000 (both from Mark Carrington, University of Cambridge, UK), polyclonal rabbit anti-*T. brucei* Rab5A serum (Field et al., 1998) 1:1000, polyclonal rabbit anti-*T. brucei* Rab11 serum (Jeffries et al., 2001) 1:1000, polyclonal rabbit anti-*T. brucei* CHC serum (Morgan et al. 2001) 1:1000, polyclonal rabbit anti-GFP serum (a gift of Michael Rout, Rockefeller University, New York, NY) 1:10,000, monoclonal anti-β-tubulin (Chemicon) 1:20,000 and monoclonal anti-HA (Roche) 1:5000. Incubations with anti-IgG rabbit horseradish peroxidase conjugates (Sigma) were performed at 1:20,000 in Tris-buffered saline containing Tween-20 and non-fat powdered milk. Detection was by chemiluminescence with luminol (Sigma) on BioMaxMR film (Kodak). For densitometry, fluorographs were scanned at 16-bit gray scale, and exposures selected where the signal was unsaturated. Exposures in figures usually represent overexposed versions of data used for quantification. Quantification was done using NIH ImageJ software (http://rsbweb.nih.gov/ij/).

### Protein turnover

Cycloheximide (Sigma) was added to log-phase cultures at a final concentration of 100 μg/ml.

### Immunofluorescence

Log-phase cells were fixed in 3% paraformaldehyde in PBS on ice and adhered to poly-L-lysine slides (Sigma). Cells were permeabilized with 0.1% Triton-X-100, washed and blocked in 20% foetal calf serum (FCS), incubated with primary antibodies for 1 hour and washed, secondary antibodies applied at 1:1000 for 1 hour, and mounted with Vectashield containing DAPI (Vectalabs). Image acquisition was performed with a Nikon Eclipse E600 epifluorescence microscope fitted with a Hamamatsu CDD digital camera and Metamorph (Molecular Devices), and processed with Photoshop (Adobe). Confocal microscopy images were acquired with a Leica TCS-NT confocal microscope with a 100× 1.4 NA objective. Images were processed with Huygens deconvolution software (Scientific Volume Imaging) and Adobe Photoshop. All images were taken under non-saturating conditions. All quantification was done using identical exposures using raw data within Metamorph. Antibodies were used at the following dilutions: *T. brucei* Rab28, 1:500; *T. brucei* Rab5A, 1:200; *T. brucei* Rab11, 1:200; *T. brucei* CHC, 1:750; *T. brucei* Rab1, 1:100; p67, 1:500; VSG-221, 1:1000; GRASP, 1:200; ISG100, 1:5; ISG75 1:5000; ISG65 1:1000; and antibodies to HA and GFP at 1:2000 and 1:2500, respectively.

### Ultrastructural analysis

$1\times10^8$ *T. brucei* Rab28$^{RNAi}$ cells were washed with 0.1 M HEPES pH 7.0, 0.98% sodium chloride and fixed for 4 hours on ice in 2% glutaraldehyde, 2 mM calcium chloride, 0.1 M PIPES buffer pH 7.4. Then, 100 μl 33% $H_2O_2$ was added to each 10 ml of fixative immediately prior to use. After three washes in 0.1 M HEPES pH 7.0, the pellet was processed for electron microscopy. Sections were viewed using a Philips CM100 electron microscope (FEI-Philips) operated at 80 kV.

### Concanavalin A and transferrin uptake

Cells were harvested, washed in serum-free media and resuspended at $5\times10^5$ cells/ml in serum-free media containing 1% BSA. Parasites were equilibrated at 37℃ for 15 minutes before addition of FITC-conjugated Concanavalin A (ConA) or transferrin–Alexa Fluor 633 conjugate (Molecular Probes) to final

concentrations of 5 μg/ml or 25 μg/ml, respectively. Aliquots of $2 \times 10^6$ cells were removed, and the uptake of fluorophore quenched by addition of ice-cold PBS. Samples were washed at 4℃ to remove excess probe. ConA samples were prepared for immunofluorescence and transferrin samples were fixed in 1% formaldehyde on ice for 10 minutes before flow cytometry on a Cyan LX-FACS (DakoCytomation). Cell-associated fluorescence from 50,000 cells was measured for Alexa Fluor 633 at 665 and 720 nm and analysed with Summit (Cytomation).

#### Transferrin export

Cells were washed to remove excess free serum components and resuspended at $5 \times 10^5$ cells/ml in serum-free media containing 1% BSA. Transferrin–Alexa Fluor 633 was added at 25 μg/ml and cells incubated at 37℃ for 1 hour to allow intracellular accumulation. Cells were washed at 4℃ to remove excess fluorophore and returned to 37℃. Cells were fixed and taken for FACS analysis.

#### Trypanosome lytic factor sensitivity

Blood was taken from fasted healthy volunteers and allowed to clot for 1 hour at 37℃ before cooling at 4℃. Serum was separated by centrifuging at 10,000 ***g*** for 20 minutes at 4℃ and heat-inactivated by incubating at 55℃ for 30 minutes. Sera were stored at −80℃. Cells were harvested, washed in serum-free media and resuspended in media supplemented with 0–20% human serum. Total serum concentration was maintained at 20% with FCS. Cells were incubated at 37℃ and cell density determined using a haemocytometer.

## Acknowledgements

We thank James Bangs, Mark Carrington and Keith Gull for various antibodies, V. Lila Koumandou for tagged cell lines and members of the Field laboratory for discussions, donation of serum and support.

## Funding

This work was funded by a studentship from the Medical Research Council (MRC), UK to J.H.L.; and Wellcome Trust project and program grants [grant numbers 082813/Z/07/Z, 09007/Z/09/Z to M.C.F.]. Deposited in PMC for release after 6 months.

## References

**Ackers, J. P., Dhir, V. and Field, M. C.** (2005). A bioinformatic analysis of the RAB genes of Trypanosoma brucei. *Mol. Biochem. Parasitol.* **141**, 89-97.

**Alexander, D. L., Schwartz, K. J., Balber, A. E. and Bangs, J. D.** (2002). Developmentally regulated trafficking of the lysosomal membrane protein p67 in Trypanosoma brucei. *J. Cell Sci.* **115**, 3253-3263.

**Allen, C. L., Goulding, D. and Field, M. C.** (2003). Clathrin-mediated endocytosis is essential in Trypanosoma brucei. *EMBO J.* **22**, 4991-5002.

**Allen, C. L., Liao, D., Chung, W. L. and Field, M. C.** (2007). Dileucine signal-dependent and AP-1-independent targeting of a lysosomal glycoprotein in Trypanosoma brucei. *Mol. Biochem. Parasitol.* **156**, 175-190.

**Alsford, S., Turner, D. J., Obado, S. O., Sanchez-Flores, A., Glover, L., Berriman, M., Hertz-Fowler, C. and Horn, D.** (2011). High-throughput phenotyping using parallel sequencing of RNA interference targets in the African trypanosome. *Genome Res.* **21**, 915-924.

**Arighi, C. N., Hartnell, L. M., Aguilar, R. C., Haft, C. R. and Bonifacino, J. S.** (2004). Role of the mammalian retromer in sorting of the cation-independent mannose 6-phosphate receptor. *J. Cell Biol.* **165**, 123-133.

**Babst, M., Odorizzi, G., Estepa, E. J. and Emr, S. D.** (2000). Mammalian tumor susceptibility gene 101 (TSG101) and the yeast homologue, Vps23p, both function in late endosomal trafficking. *Traffic* **1**, 248-258.

**Bache, K. G., Brech, A., Mehlum, A. and Stenmark, H.** (2003). Hrs regulates multivesicular body formation via ESCRT recruitment to endosomes. *J. Cell Biol.* **162**, 435-442.

**Bastin, P., Ellis, K., Kohl, L. and Gull, K.** (2000). Flagellum ontogeny in trypanosomes studied via an inherited and regulated RNA interference system. *J. Cell Sci.* **113**, 3321-3328.

**Behnia, R. and Munro, S.** (2005). Organelle identity and the signposts for membrane traffic. *Nature* **438**, 597-604.

**Belenkaya, T. Y., Wu, Y., Tang, X., Zhou, B., Cheng, L., Sharma, Y. V., Yan, D., Selva, E. M. and Lin, X.** (2008). The retromer complex influences Wnt secretion by recycling wntless from endosomes to the trans-Golgi network. *Dev. Cell* **14**, 120-131.

**Berriman, M., Ghedin, E., Hertz-Fowler, C., Blandin, G., Renauld, H., Bartholomeu, D. C., Lennard, N. J., Caler, E., Hamlin, N. E., Haas, B. et al.** (2005). The genome of the African trypanosome *Trypanosoma brucei*. *Science* **309**, 416-422.

**Brauers, A., Schurmann, A., Massmann, S., Muhl-Zurbes, P., Becker, W., Kainulainen, H., Lie, C. and Joost, H. G.** (1996). Alternative mRNA splicing of the novel GTPase Rab28 generates isoforms with different C-termini. *Eur. J. Biochem.* **237**, 833-840.

**Brickman, M. J., Cook, J. M. and Balber, A. E.** (1995). Low temperature reversibly inhibits transport from tubular endosomes to a perinuclear, acidic compartment in African trypanosomes. *J. Cell Sci.* **108**, 3611-3621.

**Brighouse, A., Dacks, J. B. and Field, M. C.** (2010). Rab protein evolution and the history of the eukaryotic endomembrane system. *Cell Mol. Life Sci.* **67**, 3449-3465.

**Cavalier-Smith, T.** (2010). Kingdoms Protozoa and Chromista and the eozoan root of the eukaryotic tree. *Biol. Lett.* **6**, 342-345.

**Chung, W. L., Carrington, M. and Field, M. C.** (2004). Cytoplasmic targeting signals in transmembrane invariant surface glycoproteins of trypanosomes. *J. Biol. Chem.* **279**, 54887-54895.

**Chung, W. L., Leung, K. F., Carrington, M. and Field, M. C.** (2008). Ubiquitylation is required for degradation of transmembrane surface proteins in trypanosomes. *Traffic* **9**, 1681-1697.

**Cross, G. A.** (1996). Antigenic variation in trypanosomes: secrets surface slowly. *Bioessays* **18**, 283-291.

**Delprato, A. and Lambright, D. G.** (2007). Structural basis for Rab GTPase activation by VPS9 domain exchange factors. *Nat. Struct. Mol. Biol.* **14**, 406-412.

**Dhir, V., Goulding, D. and Field, M. C.** (2004). TbRAB1 and TbRAB2 mediate trafficking through the early secretory pathway of *Trypanosoma brucei*. *Mol. Biochem. Parasitol.* **137**, 253-265.

**Diehl, S., Diehl, F., El-Sayed, N. M., Clayton, C. and Hoheisel, J. D.** (2002). Analysis of stage-specific gene expression in the bloodstream and the procyclic form of *Trypanosoma brucei* using a genomic DNA-microarray. *Mol. Biochem. Parasitol.* **123**, 115-123.

**Doyotte, A., Russell, M. R., Hopkins, C. R. and Woodman, P. G.** (2005). Depletion of TSG101 forms a mammalian ''Class E'' compartment: a multicisternal early endosome with multiple sorting defects. *J. Cell Sci.* **118**, 3003-3017.

**Eathiraj, S., Pan, X., Ritacco, C. and Lambright, D. G.** (2005). Structural basis of family-wide Rab GTPase recognition by rabenosyn-5. *Nature* **436**, 415-419.

**Felder, S., Miller, K., Moehren, G., Ullrich, A., Schlessinger, J. and Hopkins, C. R.** (1990). Kinase activity controls the sorting of the epidermal growth factor receptor within the multivesicular body. *Cell* **61**, 623-634.

**Field, H. and Field, M. C.** (1997). Tandem duplication of rab genes followed by sequence divergence and acquisition of distinct functions in *Trypanosoma brucei*. *J. Biol. Chem.* **272**, 10498-10505.

**Field, H., Farjah, M., Pal, A., Gull, K. and Field, M. C.** (1998). Complexity of trypanosomatid endocytosis pathways revealed by Rab4 and Rab5 isoforms in *Trypanosoma brucei*. *J. Biol. Chem.* **273**, 32102-32110.

**Field, M. C. and Carrington, M.** (2009). The trypanosome flagellar pocket. *Nat. Rev. Microbiol.* **7**, 775-786.

**Filimonenko, M., Stuffers, S., Raiborg, C., Yamamoto, A., Malerod, L., Fisher, E. M., Isaacs, A., Brech, A., Stenmark, H. and Simonsen, A.** (2007). Functional multivesicular bodies are required for autophagic clearance of protein aggregates associated with neurodegenerative disease. *J. Cell Biol.* **179**, 485-500.

**Fridberg, A., Olson, C. L., Nakayasu, E. S., Tyler, K. M., Almeida, I. C. and Engman, D. M.** (2008). Sphingolipid synthesis is necessary for kinetoplast segregation and cytokinesis in *Trypanosoma brucei*. *J. Cell Sci.* **121**, 5225-5235.

**Gabernet-Castello, C., Dacks, J. B. and Field, M. C.** (2009). The single ENTH-domain protein of trypanosomes; endocytic functions and evolutionary relationship with epsin. *Traffic* **10**, 894-911.

**Grab, D. J., Wells, C. W., Shaw, M. K., Webster, P. and Russo, D. C.** (1992). Endocytosed transferrin in African trypanosomes is delivered to lysosomes and may not be recycled. *Eur. J. Cell Biol.* **59**, 398-404.

**Grosshans, B. L., Ortiz, D. and Novick, P.** (2006). Rabs and their effectors: achieving specificity in membrane traffic. *Proc. Natl. Acad. Sci. USA* **103**, 11821-11827.

**Hager, K. M., Pierce, M. A., Moore, D. R., Tytler, E. M., Esko, J. D. and Hajduk, S. L.** (1994). Endocytosis of a cytotoxic human high density lipoprotein results in disruption of acidic intracellular vesicles and subsequent killing of African trypanosomes. *J. Cell Biol.* **126**,155-167.

**Hall, B., Allen, C. L., Goulding, D. and Field, M. C.** (2004). Both of the Rab5 subfamily small GTPases of *Trypanosoma brucei* are essential and required for endocytosis. *Mol. Biochem. Parasitol.* **138**, 67-77.

**Hammond, D. E., Carter, S., McCullough, J., Urbe, S. and Vande Woude, G.** (2003). Endosomal dynamics of Met determine signaling output. *Mol. Biol. Cell* **14**, 1346-1354.

**Hu, Y. H., Warnatz, H. J., Vanhecke, D., Wagner, F., Fiebitz, A., Thamm, S., Kahlem, P., Lehrach, H., Yaspo, M. L. and Janitz, M.** (2006). Cell array-based intracellular localization screening reveals novel functional features of human chromosome 21 proteins. *BMC Genomics* **7**, 155.

**Hung, C. H., Qiao, X., Lee, P. T. and Lee, M. G.** (2004). Clathrin-dependent targeting of receptors to the flagellar pocket of procyclic-form *Trypanosoma brucei*. *Eukaryot. Cell* **3**, 1004-1014.

**Irminger-Finger, I., Busquets, S., Calabrio, F., Lopez-Soriano, F. J. and Argiles, J. M.** (2006). BARD1 content correlates with increased DNA fragmentation associated with muscle wasting in tumour-bearing rats. *Oncol. Rep.* **15**, 1425-1428.

**Jeffries, T. R., Morgan, G. W. and Field, M. C.** (2001). A developmentally regulated rab11 homologue in *Trypanosoma brucei* is involved in recycling processes. *J. Cell Sci.* **114**, 2617-2626.

**Katzmann, D. J., Babst, M. and Emr, S. D.** (2001). Ubiquitin-dependent sorting into the multivesicular body pathway requires the function of a conserved endosomal protein sorting complex, ESCRT-I. *Cell* **106**, 145-155.

**Katzmann, D. J., Stefan, C. J., Babst, M. and Emr, S. D.** (2003). Vps27 recruits ESCRT machinery to endosomes during MVB sorting. *J. Cell Biol.* **162**, 413-423.

**Kelley, R. J., Alexander, D. L., Cowan, C., Balber, A. E. and Bangs, J. D.** (1999). Molecular cloning of p67, a lysosomal membrane glycoprotein from *Trypanosoma brucei. Mol. Biochem. Parasitol.* **98**, 17-28.

**Kelly, S., Reed, J., Kramer, S., Ellis, L., Webb, H., Sunter, J., Salje, J., Marinsek, N., Gull, K., Wickstead, B. et al.** (2007). Functional genomics in *Trypanosoma brucei:* a collection of vectors for the expression of tagged proteins from endogenous and ectopic gene loci. *Mol. Biochem. Parasitol.* **154**, 103-109.

**Kirschbaum, M. H. and Yarden, Y.** (2000). The ErbB/HER family of receptor tyrosine kinases: A potential target for chemoprevention of epithelial neoplasms. *J. Cell Biochem. Suppl.* **34**, 52-60.

**Koumandou, V. L., Natesan, S. K., Sergeenko, T. and Field, M. C.** (2008). The trypanosome transcriptome is remodelled during differentiation but displays limited responsiveness within life stages. *BMC Genomics* **9**, 298.

**Koumandou, V. L., Klute, M. J., Herman, E. K., Nunez-Miguel, R., Dacks, J. B. and Field, M. C.** (2011). Evolutionary reconstruction of the retromer complex and its function in *Trypanosoma brucei*. *J. Cell Sci.* **124**, 1496-1509.

**Langreth, S. G. and Balber, A. E.** (1975). Protein uptake and digestion in bloodstream and culture forms of *Trypanosoma brucei. J. Protozool.* **22**, 40-53.

**Lee, J. A., Beigneux, A., Ahmad, S. T., Young, S. G. and Gao, F. B.** (2007). ESCRT-III dysfunction causes autophagosome accumulation and neurodegeneration. *Curr. Biol.* **17**, 1561-1567.

**Lee, S. H., Baek, K. and Dominguez, R.** (2008). Large nucleotide-dependent conformational change in Rab28. *FEBS Lett.* **582**, 4107-4111.

**Leung, K. F., Dacks, J. B. and Field, M. C.** (2008). Evolution of the multivesicular body ESCRT machinery; retention across the eukaryotic lineage. *Traffic* **9**, 1698-1716.

**Leung, K. F., Riley, F. S., Carrington, M. and Field, M. C.** (2011). Ubiquitylation and developmental regulation of invariant surface protein expression in trypanosomes. *Eukaryot. Cell* **10**, 916-931.

**Lumb, J. H. and Field, M. C.** (2011). Rab23 is a flagellar protein in *Trypanosoma brucei. BMC Res. Notes* **4**, 190.

**Mackey, Z. B., O'Brien, T. C., Greenbaum, D. C., Blank, R. B. and McKerrow, J. H.** (2004). A cathepsin B-like protease is required for host protein degradation in *Trypanosoma brucei. J. Biol. Chem.* **279**, 48426-48433.

**Mehlert, A., Bond, C. S. and Ferguson, M. A.** (2002). The glycoforms of a *Trypanosoma brucei* variant surface glycoprotein and molecular modeling of a glycosylated surface coat. *Glycobiology* **12**, 607-612.

**Merithew, E., Hatherly, S., Dumas, J. J., Lawe, D. C., Heller-Harrison, R. and Lambright, D. G.** (2001). Structural plasticity of an invariant hydrophobic triad in the switch regions of Rab GTPases is a determinant of effector recognition. *J. Biol. Chem.* **276**, 13982-13988.

**Moberg, K. H., Schelble, S., Burdick, S. K. and Hariharan, I. K.** (2005). Mutations in erupted, the Drosophila ortholog of mammalian tumor susceptibility gene 101, elicit non-cell-autonomous overgrowth. *Dev. Cell* **9**, 699-710.

**Morgan, G. W., Allen, C. L., Jeffries, T. R., Hollinshead, M. and Field, M. C.** (2001). Developmental and morphological regulation of clathrin-mediated endocytosis in *Trypanosoma brucei. J. Cell Sci.* **114**, 2605-2615.

**Ostermeier, C. and Brunger, A. T.** (1999). Structural basis of Rab effector specificity: crystal structure of the small G protein Rab3A complexed with the effector domain of rabphilin-3A. *Cell* **96**, 363-374.

**Overath, P. and Engstler, M.** (2004). Endocytosis, membrane recycling and sorting of GPI-anchored proteins: *Trypanosoma brucei* as a model system. *Mol. Microbiol.* **53**, 735-744.

**Overath, P., Chaudhri, M., Steverding, D. and Ziegelbauer, K.** (1994). Invariant surface proteins in bloodstream forms of *Trypanosoma brucei. Parasitol. Today* **10**, 53-58.

**Pal, A., Hall, B. S., Nesbeth, D. N., Field, H. I. and Field, M. C.** (2002). Differential endocytic functions of *Trypanosoma brucei* Rab5 isoforms reveal a glycosylphosphatidylinositol-specific endosomal pathway. *J. Biol. Chem.* **277**, 9529-9539.

**Pal, A., Hall, B. S., Jeffries, T. R. and Field, M. C.** (2003). Rab5 and Rab11 mediate transferrin and anti-variant surface glycoprotein antibody recycling in *Trypanosoma brucei. Biochem. J.* **374**, 443-451.

**Pays, E., Vanhollebeke, B., Vanhamme, L., Paturiaux-Hanocq, F., Nolan, D. P. and Perez-Morga, D.** (2006). The trypanolytic factor of human serum. *Nat. Rev. Microbiol.* **4**, 477-486.

**Pereira-Leal, J. B. and Seabra, M. C.** (2001). Evolution of the Rab family of small GTP-binding proteins. *J. Mol. Biol.* **313**, 889-901.

**Perez-Morga, D., Vanhollebeke, B., Paturiaux-Hanocq, F., Nolan, D. P., Lins, L., Homble, F., Vanhamme, L., Tebabi, P., Pays, A., Poelvoorde, P. et al.** (2005). Apolipoprotein L-I promotes trypanosome lysis by forming pores in lysosomal membranes. *Science* **309**, 469-472.

**Quijada, L., Guerra-Giraldez, C., Drozdz, M., Hartmann, C., Irmer, H., Ben-Dov, C., Cristodero, M., Ding, M. and Clayton, C.** (2002). Expression of the human RNA-binding protein HuR in *Trypanosoma brucei* increases the abundance of mRNAs containing AU-rich regulatory elements. *Nucleic. Acids Res.* **30**, 4414-4424.

**Raiborg, C., Malerod, L., Pedersen, N. M. and Stenmark, H.** (2008). Differential functions of Hrs and ESCRT proteins in endocytic membrane trafficking. *Exp. Cell Res.* **314**, 801-813.

**Raper, J., Portela, M. P., Lugli, E., Frevert, U. and Tomlinson, S.** (2001). Trypanosome lytic factors: novel mediators of human innate immunity. *Curr. Opin. Microbiol.* **4**, 402-408.

**Razi, M. and Futter, C. E.** (2006). Distinct roles for Tsg101 and Hrs in multivesicular body formation and inward vesiculation. *Mol. Biol. Cell* **17**, 3469-3483.

**Redmond, S., Vadivelu, J. and Field, M. C.** (2003). RNAit: an automated web-based tool for the selection of RNAi targets in *Trypanosoma brucei. Mol. Biochem. Parasitol.* **128**, 115-118.

**Rink, J., Ghigo, E., Kalaidzidis, Y. and Zerial, M.** (2005). Rab conversion as a mechanism of progression from early to late endosomes. *Cell* **122**, 735-749.

**Seabra, M. C., Mules, E. H. and Hume, A. N.** (2002). Rab GTPases, intracellular traffic and disease. *Trends Mol. Med.* **8**, 23-30.

**Seaman, M. N.** (2004). Cargo-selective endosomal sorting for retrieval to the Golgi requires retromer. *J. Cell Biol.* **165**, 111-122.

**Seaman, M. N., McCaffery, J. M. and Emr. S. D.** (1998). A membrane coat complex essential for endosome-to-Golgi retrograde transport in yeast. *J. Cell Biol.* **142**, 665-681.

**Shorter, J., Watson, R., Giannakou, M. E., Clarke, M., Warren, G. and Barr, F. A.** (1999). GRASP55, a second mammalian GRASP protein involved in the stacking of Golgi cisternae in a cell-free system. *EMBO J.* **18**, 4949-4960.

**Stenmark, H.** (2009). Rab GTPases as coordinators of vesicle traffic. *Nat. Rev. Mol. Cell. Biol.* **10**, 513-525.

**Steverding, D., Stierhof, Y. D., Fuchs, H., Tauber, R. and Overath, P.** (1995). Transferrin-binding protein complex is the receptor for transferrin uptake in *Trypanosoma brucei. J. Cell Biol.* **131**, 1173-1182.

**Tanida, I., Minematsu-Ikeguchi, N., Ueno, T. and Kominami, E.** (2005). Lysosomal turnover, but not a cellular level, of endogenous LC3 is a marker for autophagy. *Autophagy* **1**, 84-91.

**Thompson, B. J., Mathieu, J., Sung, H. H., Loeser, E., Rorth, P. and Cohen, S. M.** (2005). Tumor suppressor properties of the ESCRT-II complex component Vps25 in Drosophila. *Dev. Cell.* **9**, 711-720.

**Vaccari, T. and Bilder, D.** (2005). The Drosophila tumor suppressor vps25 prevents nonautonomous overproliferation by regulating notch trafficking. *Dev. Cell.* **9**, 687-698.

**van Deurs, B., Holm, P. K., Kayser, L., Sandvig, K. and Hansen, S. H.** (1993). Multivesicular bodies in HEp-2 cells are maturing endosomes. *Eur. J. Cell Biol.* **61**, 208-224.

**Vanhollebeke, B., De Muylder, G., Nielsen, M. J., Pays, A., Tebabi, P., Dieu, M., Raes, M., Moestrup, S. K. and Pays, E.** (2008). A haptoglobin-hemoglobin receptor conveys innate immunity to *Trypanosoma brucei* in humans. *Science* **320**, 677-681.

**Webster, P. and Grab, D. J.** (1988). Intracellular colocalization of variant surface glycoprotein and transferrin-gold in *Trypanosoma brucei. J. Cell Biol.* **106**, 279-288.

**Wirtz, E., Leal, S., Ochatt, C. and Cross, G. A.** (1999). A tightly regulated inducible expression system for conditional gene knock-outs and dominant-negative genetics in *Trypanosoma brucei. Mol. Biochem. Parasitol.* **99**, 89-101.

**Wollert, T. and Hurley, J. H.** (2010). Molecular mechanism of multivesicular body biogenesis by ESCRT complexes. *Nature* **464**, 864-869.

**Yang, R., Frank, B., Hemminki, K., Bartram, C. R., Wappenschmidt, B., Sutter, C., Kiechle, M., Bugert, P., Schmutzler, R. K., Arnold, N. et al.** (2008). SNPs in ultraconserved elements and familial breast cancer risk. *Carcinogenesis* **29**, 351-355.